Floral asymmetry involves an interplay between TCP and MYB transcription factors in *Antirrhinum*

Susie B. Corley, Rosemary Carpenter, Lucy Copsey, and Enrico Coen*

Department of Cell and Developmental Biology, John Innes Centre, Colney Lane, Norwich NR4 7UH, United Kingdom

Contributed by Enrico Coen, February 16, 2005

To understand how genes control floral asymmetry, we have isolated and analyzed the role of the *RADIALIS* (*RAD*) gene in *Antirrhinum*. We show that the *RAD* gene encodes a small MYB-like protein that is specifically expressed in the dorsal region of developing flowers. RAD has a single MYB-like domain that is closely related to one of the two MYB-like domains of DIV, a protein that has an antagonistic effect to RAD on floral development. Interactions between *RAD* and other genes indicate that floral asymmetry depends on the interplay between two pairs of transcription factors. First, a pair of TCP proteins is expressed in dorsal regions of the floral meristem, leading to the activation of *RAD* in the dorsal domain. The RAD MYB-like protein then antagonizes the related DIV MYB-like protein, preventing DIV activity in dorsal regions. In addition to its role in dorsal regions, RAD acts nonautonomously on lateral regions either directly, through RAD protein movement, or indirectly, through a signaling molecule.

flower development | dorsal | ventral | adaxial | petal shape

Floral asymmetry is thought to have evolved many times independently as a specialized mechanism for pollinator interaction (1–3). In a few cases, most notably in *Antirrhinum majus*, the molecular genetic basis of floral asymmetry has begun to be understood. Four key genes have been shown to control dorsoventral asymmetry in *Antirrhinum*: *CYCLOIDEA* (*CYC*), *DICHOTOMA* (*DICH*), *RADIALIS* (*RAD*), and *DIVARICATA* (*DIV*) (4–8). Two of these genes, *CYC* and *DICH*, promote dorsal identity and encode proteins belonging to the TCP family of transcription factors. *DIV* promotes ventral identity and encodes a protein belonging to the MYB family of transcription factors, carrying two MYB-like domains. However, the mechanism by which *CYC*, *DICH*, and *DIV* interact remains unclear. To address this question, we have isolated and characterized *RAD*, the fourth member of this group of genes, and explored how it acts in combination with the other genes to establish floral asymmetry.

Flowers of wild-type *Antirrhinum* are zygomorphic, having a single plane of symmetry (bilateral symmetry), in contrast to actinomorphic flowers, which have multiple planes of symmetry (radial symmetry) (3). The zygomorphy of *Antirrhinum* flowers reflects morphological distinctions between the upper (dorsal) and lower (lateral and ventral) organs of whorls two and three. In whorl two, each flower has two dorsal petals, two lateral petals, and one ventral petal, whereas whorl three comprises a single arrested dorsal stamen (staminode), two lateral stamens, and two ventral stamens (Fig. 1 *a* and *b*).

The *CYC* and *DICH* genes are required for dorsoventral asymmetry in *Antirrhinum* and are expressed from an early stage in the dorsal domain of the floral meristem (5, 7, 9). At later stages, *CYC* expression persists throughout most of the dorsal domain, whereas *DICH* becomes restricted to the most dorsal half of the dorsal domain. Inactivation of both *CYC* and *DICH* results in peloric (radially symmetrical) flowers, in which all petals have ventral identity (Fig. 1*h*). In *cyc* or *dich* single mutants, flowers are only partially ventralized, indicating that *CYC* and *DICH* act in a partially redundant manner (5, 7). Although *CYC* is expressed specifically in dorsal regions, it also acts nonautonomously on organs in lateral positions, because these organs are ventralized in *cyc* mutants.

A major mechanism by which *CYC* and *DICH* act is by repression of *DIV*, a gene that promotes ventral identity (6, 8). In the absence of *CYC*, *DICH*, and *DIV* (i.e., in *cyc dich div* triple mutants), all petals develop with lateral identity, whereas in the absence of just *CYC* and *DICH* (*cyc dich* double mutants), all petals have ventral identity. This observation indicates that, in a *cyc dich* background, *DIV* promotes ventral identity at all positions around the flower. In wild type, expression of *CYC* and *DICH* in dorsal regions restricts *DIV* function to the ventral and adjacent lateral domains (i.e., only these domains are affected in *div* single mutants). The effect of *CYC* and *DICH* on *DIV* appears to be posttranscriptional, because *DIV* is expressed throughout the wild-type flower at early stages in development in a pattern that is unaffected by *cyc* or *dich* mutations. At later stages, *DIV* is still expressed in all petals, although expression is enhanced in some ventral regions in a manner that depends on *DIV* itself (8).

RAD, like *CYC* and *DICH*, promotes dorsal identity, with recessive *rad* alleles giving very similar phenotypes to *cyc* alleles. This similarity, together with the linkage between *RAD* and *CYC*, led to an original assignment of *rad* and *cyc* mutations to the same locus (10). Subsequent analysis showed that the mutations fall into two complementation groups (11).

Here, we describe the isolation and characterization of *RAD*. We show that *RAD* is activated by *CYC* and *DICH* in the dorsal region of the developing flower, where it plays a major role in establishing floral asymmetry. *RAD* encodes a 93-aa protein containing a single MYB-like domain. The RAD protein is closely related to the N-terminal MYB-like domain of DIV, suggesting that RAD may have been derived from a DIV-like ancestral protein through C-terminal deletion. The molecular similarity between RAD and DIV suggests that their antagonistic phenotypic effects arise through competition for common DNA or protein targets. The RAD protein also mediates the nonautonomous effects of *CYC*, acting as a direct or indirect signal between dorsal and lateral domains.

Materials and Methods

Plant Material. The rad^{rad} and rad^{hemi} lines, originally named cyc^{rad} and cyc^{hemi}, were obtained from the Gatersleben seed bank (lines 80 and 78) (12). The other alleles arose from transposon mutagenesis carried out at the John Innes Centre. The *rad-609* and *rad-654* alleles arose from the wild-type line JI-stock 75 (11), and the *rad-689* allele arose from a *centroradialis* (*cen*) mutant line (JI-stock 663) (13). The *cyc-608* and *div-35* alleles used to create double mutants are described in refs. 8 and 11.

DNA Methods. Genomic DNA was extracted from *A. majus* leaf tissue, as described in ref. 14. Southern analyses were carried out

Abbreviations: *CYC*, *CYCLOIDEA*; *DICH*, *DICHOTOMA*; *DIV*, *DIVARICATA*; *RAD*, *RADIALIS*.

Data deposition: The sequence reported in this paper has been deposited in the GenBank database (accession no. AY954971).

*To whom correspondence should be addressed. E-mail: enrico.coen@bbsrc.ac.uk.

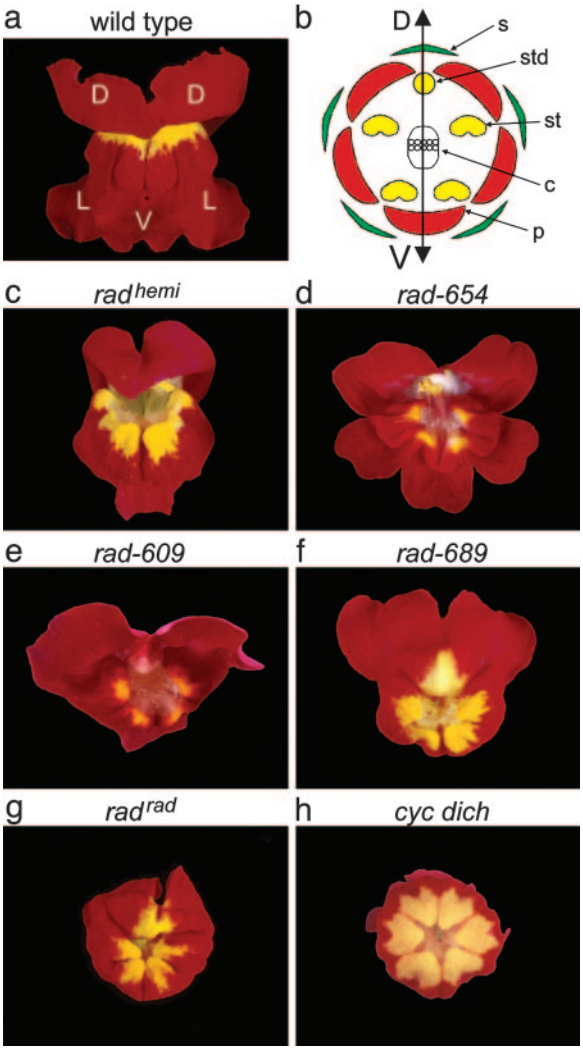

Fig. 1. Phenotype of *rad* mutants compared with wild type and a peloric mutant. (*a*) Frontal view of a wild-type *Antirrhinum* flower. D, dorsal petal; L, lateral petal; V, ventral petal. (*b*) Diagram showing the four whorls of the wild-type *Antirrhinum* flower. Whorl one, sepals (s); whorl two, petals (p); whorl three, stamens (st) and staminode (std); whorl four, carpels (c). The double-ended arrow marks the dorsal–ventral (DV) axis of the flower. (*c–g*) Frontal views of the five *rad* mutant lines used in this study. Note the similarity between the *rad*^{rad} flower (*g*) and the peloric *cyc dich* double mutant (*h*).

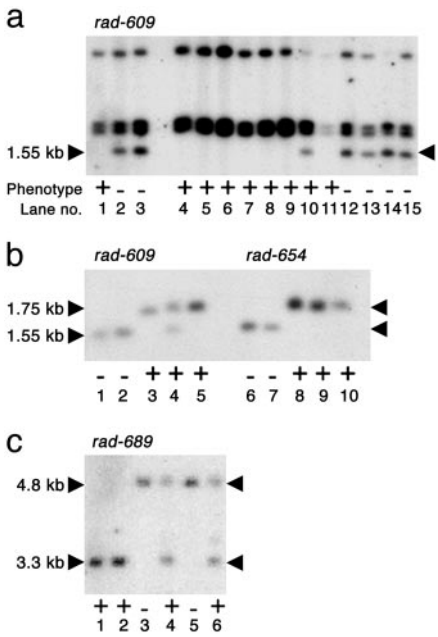

Fig. 2. Retrotransposon tagging the *RAD* locus. (*a*) Genomic DNA from *rad-609* mutants and wild-type siblings digested with *Eco*RI and probed with the 3′ end of Ram1. The segregating 1.55-kb band is marked. The wild-type plant used in lane 10 was later shown to be a heterozygote (*b*, lane 4). Lanes 1, 10, and 11 contain DNA from wild-type siblings of the original mutant plant, whereas lane 2 and lanes 12–15 contain DNA from mutant siblings. Lane 3 contains DNA from a family of *rad-609* mutants, and lanes 4–9 contain DNA from siblings of the wild-type progenitor of *rad-609*. (*b*) Genomic DNA from *rad-609* and *rad-654* mutants and their wild-type relatives digested with *Eco*RI and probed with the 215-bp sequence flanking the Ram1 insertion. The 1.75-kb wild-type bands and the 1.55-kb mutant bands are indicated. DNA in lanes 1–5 corresponds to that in lanes 3, 2, 1, 10, and 5 of *a*. Lanes 6 and 7 contain DNA from *rad-654* mutants. Lanes 8–10 contain DNA from homozygous revertants of *rad*-654. (*c*) Genomic DNA from *rad-689* mutants and their wild-type relatives digested with *Hin*dIII and probed with the 215-bp sequence flanking Ram1. The wild-type band is 3.3 kb, and the mutant band is 4.8 kb. Lanes 1 and 2 contain DNA from wild-type siblings of the original mutant. Lanes 3 and 5 contain DNA from *rad-609* mutants. DNA from heterozygous revertant siblings of these mutants was used in lanes 4 and 6. Plant phenotypes are + for wild type and − for mutant.

by using Hybond-N$^+$ nylon membranes according to the manufacturer's protocol (Amersham Pharmacia Biotech). Probes were radiolabeled with [α-^{32}P]CTP by using a kit from Amersham Pharmacia Biotech that was based on the random hexamer labeling method.

The inverse PCR method used was based on the approach described in ref. 15. Genomic DNA (≈2 μg) was digested with the appropriate restriction enzyme in 50-μl reactions. The digested DNA was extracted from the reaction by using the Wizard DNA Clean-Up System kit (Promega). The restricted fragments (≈500 ng) were then incubated overnight with T4 DNA ligase in 100-μl reactions at 12°C. The resulting circularized DNA fragments were used as templates in a PCR-based reaction on the Expand Long Template PCR System (Boehringer Mannheim) protocol. Between 10 and 20 μl of the ligation reaction was used in a 50-μl PCR mix. The PCR products were fractionated on an agarose gel, allowing the correct product to be identified, gel extracted, and ligated into the pGEM-T vector (Promega).

The segregating 1.55-kb *Eco*RI fragment seen in Fig. 2*a* was isolated by inverse PCR with primers designed against Ram1: oligo 4325 (5′-TAAGGAAGCTTCGGGTCCGG-3′) and oligo 4327 (5′-TAGGACCATGATCCCCTAGCC-3′). The resulting clone was named pJAM2255.

The 3.3-kb *Hin*dIII wild-type genomic fragment seen in Fig. 2*c* was also isolated by inverse PCR. The primers used were designed against the 215-bp fragment of the *RAD* locus that formed part of pJAM2255: oligo 4468 (5′-GTACATCATTAATATACCAC-3′) and oligo 4470 (5′-CAGTTTGTACAAACGGTTCG-3′). The resulting clone was labeled pJAM2247.

The pJAM2247 insert was used to screen a cDNA library made from young inflorescences of wild-type *A. majus* plants (16). Approximately 5 × 10^5 plaque-forming units were transferred to nitrocellulose filters (Sartorius) and probed. Six positives were obtained, all representing the same gene. The longest insert was 696 bp, and this insert was subcloned into the BlueScript KS+ vector (Stratagene) to give pJAM2246. A poly(A) tail was present in the same position in all six cDNA clones. A putative polyadenylation signal (i.e., AATAAA) was also identified, ≈20 bp upstream of the poly(A) region.

Sequence analysis was carried out by using the program

DEVELOPMENTAL BIOLOGY

WISCONSIN PACKAGE 9.0 (Genetics Computer Group, Madison, WI) in UNIX.

RNA Methods. RNA *in situ* hybridizations were carried out as described in ref. 17. Riboprobes against *RAD*, *CYC*, and *DICH* were synthesized by using plasmids pJAM2251, pJAM193, and pJAM2143, respectively. Plasmid pJAM2251 consisted of the pGEM-T vector (Promega), containing ≈370 bp of *RAD* cDNA as insert. This insert was obtained by PCR with oligos 5045 (5′-ATGGCTTCGACTCGTGGTTCTG-3′) and 5041 (5′-GAACGATTACAAACGGGTAGG-3′), by using pJAM2246 as template. Antisense probes were obtained by linearizing pJAM2251 with *Pst*I, followed by transcription from the T7 promoter. Sense probes were obtained in the same way but from another plasmid, pJAM2248. This plasmid contained the same insert as pJAM2251 but in the opposite orientation. Plasmids pJAM193 and pJAM2143 are described in refs. 5 and 7.

Results

***RAD* Mutant Phenotypes and Interactions.** Five recessive *rad*-mutant alleles were analyzed: $rad^{hemiradialis}$ (rad^{hemi}), *rad-654*, *rad-609*, *rad-689*, and $rad^{radialis}$ (rad^{rad}) (Fig. 1 *c–g*). Two of these alleles (rad^{rad} and rad^{hemi}) were originally isolated in the early 20th century by Erwin Baur (18), whereas the other alleles arose more recently from transposon mutagenesis experiments (11). Based on their phenotypes, the alleles could be arranged in a series, going from weakest to strongest in the order $rad^{hemi} < rad\text{-}609 \sim rad\text{-}654 < rad\text{-}689 < rad^{rad}$. The strongest allele, rad^{rad}, gave almost peloric (i.e., radially symmetric) flowers in which all petals resembled the ventral petal of wild type, with only the dorsal half of each dorsal petal retaining some dorsal/lateral features (petal lobes are shown schematically in Fig. 3*b*). Weaker alleles showed more partial ventralization, as illustrated schematically for *rad-609* (Fig. 3*c*). Unlike *cyc* mutants, which often have six instead of five organs per whorl, the organ number was not affected in *rad* mutants. The dorsal stamen (staminode) of *rad* mutants was typically longer than that of wild type but did not develop into the functional stamen found in *cyc* mutants (data not shown).

To investigate how *RAD* interacts with other genes in controlling floral asymmetry, several double mutants were constructed. The *rad cyc* double mutant had a fully ventralized phenotype (data not shown), even though both the *rad* and *cyc* alleles used (*rad-609* and *cyc-608*) were of intermediate strength. This result indicates that the residual asymmetry seen in *rad* single mutants depends on *CYC* activity. The double mutant between *rad-609* and a putative null *div* allele, *div-35* [*div-35* carries a frame-shift mutation (8)], had features of both the *rad-609* and *div-35* single mutants (Fig. 3 *c–e*). The petals in lateral and ventral positions were bilaterally symmetrical (as in *rad*-609) but resembled the ventral petal of *div-35* mutants, although the petals had a slightly different shape. The petals in dorsal positions had some dorsal identity but were clearly distinct from the dorsal petals of both single mutants.

Molecular Cloning of *RAD*. The *rad-609* allele arose from a transposon mutagenesis experiment, but, unlike many other transposon-induced mutations, the *rad-609* allele appeared to be genetically stable (11). One possibility was that *rad-609* was caused by insertion of a DNA sequence, such as a retrotransposon, that did not normally excise. A stable mutation caused by insertion of a retrotransposon, Ram1, had previously been described for the *incolorata* locus of *Antirrhinum* [*inc-713* (19)]. To test whether Ram1 might also be responsible for *rad-609*, DNA from *rad-609* mutants and wild-type siblings was digested with *Eco*RI, blotted, and probed with the 3′ end of Ram1, revealing a 1.55-kb *Eco*RI fragment that segregated with the *rad-609* mutant allele (Fig. 2*a*).

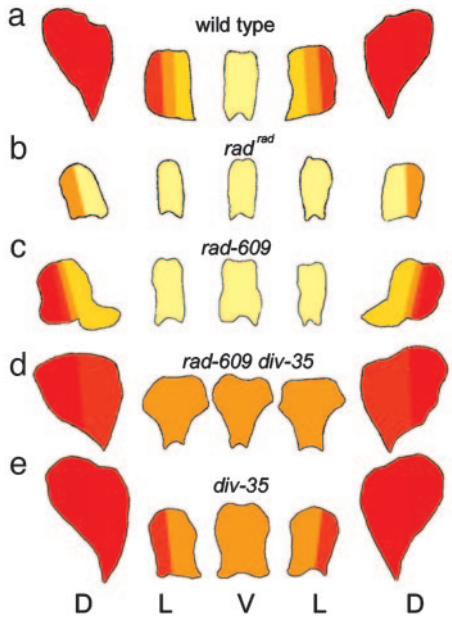

Fig. 3. Shape of petal lobes. Flowers of wild type (*a*), rad^{rad} (*b*), *rad*-609 (*c*), *rad*-609 *div-35* double mutant (*d*), and *div-35* (*e*) are shown. For each flower, the petal lobes have been laid out from left to right in positional order, starting from the right dorsal petal lobe (as shown in Fig. 1*a*) and working clockwise around the flower. The colors represent the identities of the petals based on cell types and appearance. Pale yellow represents ventral identity, and each color change from yellow to red represents a shift toward more dorsal identity (dark red). D, dorsal; L, lateral; and V, ventral.

To determine whether the 1.55-kb fragment was derived from the *RAD* locus, the fragment was amplified by inverse PCR and sequenced. In addition to Ram1, the 1.55-kb fragment contained 215 bp of flanking sequence. This 215-bp sequence was amplified and used to probe DNA from three independent *rad* mutants (*rad-609*, *rad-654*, and *rad-689*) and various wild-type lines, including some revertants derived from *rad-654* and *rad-689* (Fig. 2 *b* and *c*). A distinct band was observed in each of the *rad* mutants when compared with their wild-type relatives and revertants (some of the wild types were heterozygous, as expected from the recessive nature of *rad* alleles). This observation indicated that the 215-bp sequence flanking Ram1 was derived from the *RAD* locus.

Oligonucleotides were designed, based on the 215-bp sequence, to obtain more of the *RAD* locus by inverse PCR, leading to the amplification of a 3.3-kb *Hin*dIII genomic fragment from wild-type DNA. The fragment was sequenced and used to probe a cDNA library made from *A. majus* inflorescence RNA. Six cDNA clones were isolated, representing transcripts from a single gene. Comparison of the cDNA with the genomic sequence showed that the cDNAs were derived from a gene with an intron of 829 bp (Fig. 4*a*). There was a single large ORF, mostly in the first exon, encoding a protein of 93 aa (Fig. 4*b*).

A combination of DNA blotting and PCR was used to characterize the *rad* mutants (Fig. 4*a*). *rad-609* had a Ram1-like insertion of ≈1.45 kb within the intron. *rad-654* had an insertion of a ≈4.3-kb transposon belonging to the CACTA family (20, 21) within the intron. The similarity of the *rad-654* and *rad-609* insertion sites may account for their similar phenotypes. *rad-689* and rad^{rad} had insertions within or near the 5′ untranslated region.

***RAD* Encodes a Putative MYB-Like Protein.** Database searches revealed that the protein encoded by *RAD* is related to the MYB family of transcription factors (Fig. 4*c*). The MYB family is one

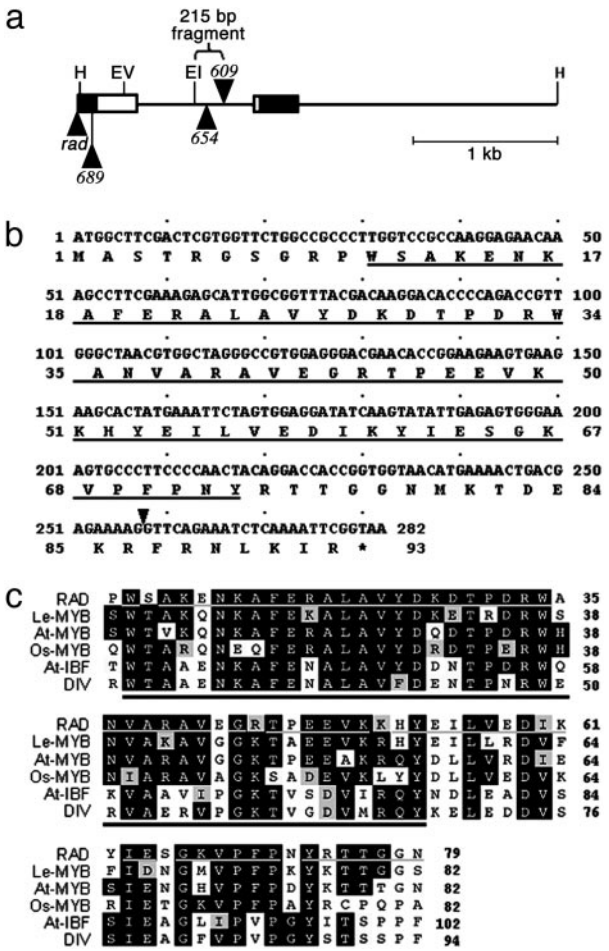

Fig. 4. The *RAD* locus, coding sequence, and predicted protein sequence. (*a*) Diagram of the 3.3-kb wild-type *Hin*dIII fragment, containing part of the *RAD* locus. The two exons are shown as boxes; white sections are coding regions, and black sections are 5′ and 3′ untranslated regions. The insertions in *rad*^{rad}, *rad-689*, *rad-654*, and *rad-609* are shown as black triangles. Also marked is the 215-bp fragment used to generate probes for Southern analysis. H, *Hin*dIII; EV, *Eco*RV; EI, *Eco*RI. (*b*) The complete coding sequence of the *RAD* gene with the predicted RAD protein sequence. The underlined amino acid sequence is similar to the MYB I domain of DIV defined in ref. 8. The black arrowhead marks the position of the intron. (*c*) Alignment of RAD, DIV, and RAD-like protein sequences. Conserved residues are shown as white letters on a black background. Residues that show similarity to the consensus are highlighted in varying shades of gray according to how similar they are. The black bar marks the conserved MYB I domain, and the gray bar indicates those amino acids in RAD that are found in at least one other sequence in the group. RAD, *A. majus* RADIALIS protein; Le-MYB, *Lycopersicon esculentum* MYB-related protein (CAB91874); At-MYB, *Arabidopsis thaliana* MYB-related protein (At2g21650; AAP40504); Os-MYB, *Oryza sativa* MYB-related protein (BAB90739); At-IBF, *A. thaliana* I box-binding-factor-like protein (At5g58900; BAB09635); DIV, *A. majus* MYB-like transcription factor DIVARICATA protein (AAL78741).

of the largest transcription factor families in plants, comprising >125 members in *Arabidopsis* (22). The diagnostic feature of this family is an ≈50-aa sequence, the MYB domain, with three tryptophan residues spaced 18–20 residues apart. In plants, one or more of the tryptophan residues may be replaced by another aromatic residue or by a similarly sized aliphatic residue. The MYB domain may be present once, twice, or three times in the protein.

RAD had a single MYB-like domain and was most closely related to a subfamily of single-repeat MYB-like proteins. Other members of this subfamily can be found in several dicots, as well as in monocots, although the function of these subfamily members is not known (e.g., Fig. 4*c*). The nearest relatives to RAD outside the subfamily are a group of proteins with two MYB-like domains that includes the *Antirrhinum* DIV protein. Of the two domains in DIV, the 63-aa MYB I region is most similar to RAD (≈52% identical; Fig. 4*c*). Because RAD is only 93 aa long, this MYB I-like domain comprises about two-thirds of the RAD protein. No other known functional domains or motifs were identified in the RAD protein sequence.

Expression of *RAD* in Wild-Type Inflorescences. To determine the expression pattern of *RAD*, RNA *in situ* hybridizations were carried out on sections from wild-type inflorescences. Floral meristems of *Antirrhinum* are generated at regular time intervals, termed plastochrons, on the periphery of the inflorescence apex. Flower development has been divided into 15 stages, each stage lasting ≈4 plastochrons (≈40 h), when plants are grown at 25°C (23, 24). The earliest clear sign of *RAD* expression was at early stage two (plastochrons 7 and 8), when the floral meristem comprised a loaf-shaped bulge of cells (Fig. 5*a*). Expression was in the dorsal region of the floral meristem. This pattern is similar to the pattern of *CYC* and *DICH* expression; although, unlike *RAD*, expression of these genes can also be detected earlier, in stage-one meristems (5).

At stage four, when sepal primordia had emerged around the meristem dome, *RAD* expression could be seen in the dorsal sepal primordium (Fig. 5*b*). Probing an adjacent section with *CYC* revealed that *CYC* was expressed in a domain that was similar to *RAD* but also extended into dorsal regions of whorls two and three (Fig. 5*c*). By stage five, *RAD* expression could be detected in the dorsal sepal and in the dorsal part of the lateral sepals, similar to the expression pattern of *CYC* at this stage (5). Also by stage five, *RAD* expression could be detected in emerging dorsal primordia of whorls two and three, suggesting that *RAD* is activated shortly after *CYC* in internal whorls (Fig. 5*d*).

In older flower buds (stages seven and eight), *RAD* expression was found mainly in the dorsal petals and staminode (Fig. 5*e*). The base of the dorsal sepal also showed weak expression. Transverse sections through these flower buds revealed that the *CYC* and *RAD* expression patterns were very similar. Except for a region at their lateral edges, both genes were expressed throughout the dorsal petals (Fig. 5 *e* and *f*). Also, both genes were expressed in the staminode; although, within the staminode, the *CYC* and *RAD* expression domains seemed almost complementary: *CYC* was expressed throughout the staminode, except for a small patch on the abaxial side, whereas *RAD* expression appeared to be strongest on the abaxial side (Fig. 5 *e* and *f*) (25).

Expression of *RAD* in Floral Symmetry Mutants. The dorsal-specific expression pattern observed for both *RAD* and *CYC* raised the question of whether these genes might influence each other's expression. To address this question, RNA *in situ* hybridizations were carried out on *cyc* and *rad* mutant inflorescences by using *RAD* and *CYC* probes, respectively. The expression pattern of *CYC* was unaffected in *rad* mutants (data not shown). However, expression of *RAD* was reduced in *cyc* mutants, being restricted to the most dorsal part of the dorsal-petal primordia (Fig. 5*h*), in contrast to wild type, where *RAD* was expressed throughout most of the dorsal-petal primordia (Fig. 5*e*). In addition, *RAD* expression was delayed in *cyc* mutants: The earliest signal was observed at about plastochrons 11 and 12 (early stage three), compared with plastochrons 7 and 8 (early stage two) in wild type. Expression of *RAD* in the dorsal stamen appeared to be unaffected in *cyc* mutants.

These results show that the loss of *CYC* activity leads to a reduction in *RAD* expression in the dorsal domains of the flower. To test whether gain of *CYC* might lead to a corresponding

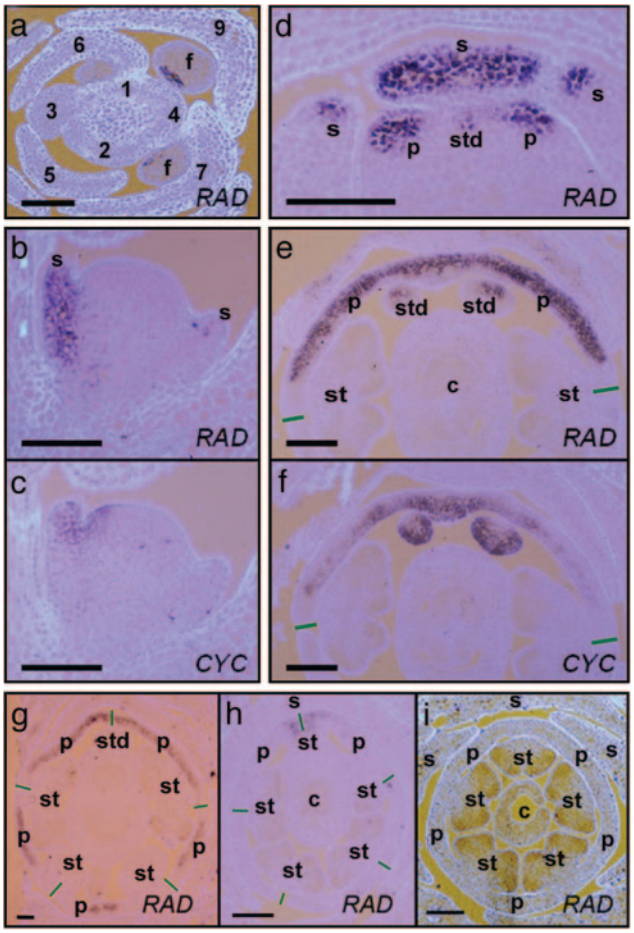

Fig. 5. RNA *in situ* hybridizations by using DIG-labeled *CYC* and *RAD* riboprobes on sections from wild-type and mutant inflorescences. (*a*) Transverse section through the tip of a wild-type inflorescence, hybridized with antisense *RAD*. Approximate plastochron numbers are marked. Early *RAD* expression can be seen in floral (f) meristems at plastochrons 7 and 9. The main stem is in the center of the picture. (*b* and *c*) Adjacent longitudinal sections through a stage-four wild-type floral meristem. The section in *b* was hybridized with antisense *RAD*, and the section in *c* was hybridized with antisense *CYC*. The main stem is on the left-hand side of the photos, and the subtending bract is on the right. (*d*) Transverse section through an early stage-five wild-type floral meristem hybridized with antisense *RAD*. Only the dorsal part of the flower (where *RAD* is expressed) is shown. (*e* and *f*) Adjacent transverse sections through a stage-seven to -eight wild-type floral meristem. The section in *e* was hybridized with antisense *RAD*, and the section in *f* was hybridized with antisense *CYC*. Only the dorsal part of the flower is shown. Green lines mark the approximate site of the junction between dorsal and lateral petals. (*g*) Transverse section from a stage-seven to -eight backpetals floral meristem. Green lines mark the approximate site of the junctions between the five petals. (*h*) Transverse section from a stage-seven *cyc-608* floral meristem. Green lines mark the approximate site of the junctions between the five petals. (*i*) Transverse section from a stage-seven *cyc dich* double-mutant floral meristem. The sections were photographed under UV light. Light blue/mauve color is calcofluor-stained tissue; dark purple/black color corresponds to DIG-labeled probe. (Scale bars, 100 μm.) s, sepal; p, petal; st, stamen; std, staminode; c, carpel.

increase of *RAD* expression, RNA *in situ* experiments were carried out on the backpetals mutant *cyc-705*. This allele confers a dorsalized phenotype and carries a transposon insertion in the *CYC* promoter that results in ectopic expression of *CYC* in the lateral and ventral petals after about stage six (7, 25). *RAD* was also ectopically expressed in lateral and ventral petals of the backpetals mutant, mirroring the ectopic pattern of *CYC* expression (Fig. 5*g*).

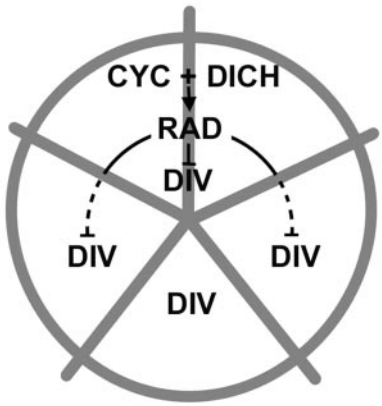

Fig. 6. Model for interactions between genes controlling dorsoventral asymmetry. Expression of *CYC* and *DICH* in the dorsal domain (upper two sections) leads to activation of *RAD* (solid arrow), which, in turn, inhibits *DIV* activity in both dorsal regions (solid line) and in lateral regions (dotted line).

Although *RAD* expression was reduced in *cyc* mutants, residual expression was still observed in dorsal-petal primordia, suggesting that a gene other than *CYC* could also be involved in activating *RAD* in a dorsal-specific manner. A good candidate was *DICH,* because this gene is expressed in the domain where residual *RAD* expression is observed [i.e., in the most dorsal region of the dorsal-petal primordia (7)]. To test whether *DICH* might be involved, RNA *in situ* hybridizations were carried out on *cyc dich* double mutants by using the *RAD* probe. No *RAD* transcripts could be detected at any stage of floral development of double mutants, indicating that *DICH* acted partially redundantly with *CYC* to regulate *RAD* expression (Fig. 5*i*). Probing *dich* single mutants with *RAD* revealed no obvious reduction in expression compared with that in wild type, showing that *DICH* had less impact than *CYC* on *RAD* expression, consistent with the weaker phenotypic effects of *dich* compared with *cyc* mutations.

RNA *in situ* hybridization was also carried out on *div*-mutant floral meristems by using the *RAD* probe. Mutations in *DIV* appeared to have no effect on *RAD* expression (data not shown).

Discussion

***RAD* Encodes a Small MYB Protein.** As with the other three genes controlling dorsoventral asymmetry in *Antirrhinum*, *RAD* encodes a protein belonging to a transcription-factor family. However, unlike the dorsal promoting genes *CYC* and *DICH*, the protein encoded by *RAD* is not a member of the TCP family. Rather, this protein belongs to the MYB superfamily of transcription factors, being closely related to DIV, which has the opposite function of *RAD* in promoting ventral identity. These results raise the question of how two pairs of proteins, two TCP proteins and two MYB-like proteins, interact to control floral asymmetry.

***CYC* and *DICH* Activate *RAD*.** Several pieces of evidence suggest that a major mechanism by which *CYC* and *DICH* influence petal development is through activation of *RAD* (Fig. 6). (*i*) *RAD* is activated in a similar domain to that of *CYC* and *DICH*, in dorsal regions of the developing flower bud. (*ii*) Activation of *RAD* occurs shortly after that of *CYC* and *DICH*. (*iii*) Activation of *RAD* depends on both *CYC* and *DICH* function: Expression of *RAD* is reduced in floral meristems of the *cyc* single mutant and disappears altogether in the *cyc dich* double mutant. (*iv*) Ectopic expression of *CYC* is sufficient to activate *RAD* in lateral and ventral petals, resulting in a dorsalized phenotype. (*v*) The petal phenotype of strong *rad* mutants resembles that of the *cyc dich*

double mutant. Because both *CYC* and *DICH* encode proteins belonging to the TCP family of transcription factors, it is possible that *CYC* and *DICH* activate *RAD* directly by binding to its regulatory regions or indirectly through activation of an intermediary gene. Once activated, *RAD* may act on downstream target genes independently of *CYC/DICH*, or its action may require the continuing presence of *CYC* and *DICH*.

If all the effects of *CYC* and *DICH* are mediated through *RAD*, then the loss-of-function *rad* mutant flowers should be identical to *cyc dich* double mutant flowers. The strongest *rad* mutant phenotypes identified so far, although very similar to the *cyc dich* phenotype, differ in several respects. Unlike *cyc dich* mutants, strong *rad* mutant flowers have slightly asymmetric dorsal petals, do not have fully functional stamens in dorsal positions, and have five organs per whorl rather than six. It is possible that the strong *rad* alleles obtained so far do not result in complete loss of function and that the distinctions from *cyc dich* are simply due to residual *RAD* activity. Alternatively, some of the effects of *CYC/DICH* may not be mediated by *RAD*. Some support for such a *RAD*-independent mechanism comes from the observation that *cyc-608 rad-609* double mutants have fully ventralized flowers, showing that the residual asymmetry of *rad* mutants is lost if *cyc* is also mutated. *CYC* could therefore be controlling floral asymmetry independently of *RAD* as well as through *RAD*.

***RAD* May Act, in Part, by Inhibiting *DIV*.** At a morphological level, *RAD* and *DIV* have apparently antagonistic functions: *RAD* promotes dorsal identity, whereas *DIV* promotes ventral identity. Given the sequence similarity between the RAD and DIV proteins, this antagonism most likely reflects molecular competition. DIV is a 307-aa protein with two MYB-like domains (I and II) resembling other functional MYB transcription activators (26), whereas RAD is a 93-aa protein with a single MYB I-like domain. RAD may therefore have been derived from a DIV-like ancestor through loss of the C-terminal MYB II domain, reducing the protein's functionality. Although not fully functional as a transcriptional activator, RAD could nevertheless inhibit DIV by competitively binding to DIV's target sequences or to proteins that interact with DIV. Expression of *RAD* in dorsal petals would therefore prevent DIV protein from functioning in these regions. This mechanism would account for the effects of *DIV* being restricted to lateral and ventral petals, even though *DIV* is expressed in all petals (8).

Although antagonism of *DIV* may be a key mechanism for *RAD* influencing floral asymmetry, this antagonism does not account for all aspects of *RAD* function, because null *div* mutants still have asymmetric flowers with distinctive dorsal petals (8). Moreover, *rad div* double mutants have a phenotype distinct from that of *div* single mutants. *RAD* must therefore be able to influence development in ways other than by antagonizing *DIV*, perhaps by interfering with the action of other members of the MYB family of transcription factors.

Nonautonomous Effects of *CYC* and *RAD*. The precise alignment of *CYC* and *RAD* expression in dorsal petals indicates that *CYC* can activate *RAD* in an autonomous manner. The nonautonomous effect of *CYC* on lateral petals is therefore likely to be downstream of *RAD* activation. One possibility is that activation of *RAD* in dorsal regions influences the production of a downstream signaling molecule that, in turn, influences development in lateral positions. Alternatively, the RAD protein may move from cells in the dorsal domain to those in the lateral domain. Nonautonomous gene action mediated by cell-to-cell protein movement has been described for plants (e.g., ref. 27). A case of particular relevance involves the *Arabidopsis* CAPRICE (CPC) protein, a single-repeat MYB-like protein of a size similar to RAD (94 aa, compared with 93 aa for RAD). The *CPC* gene is expressed in only nonhair cells in wild-type roots, but the CPC protein can also be detected in adjacent hair cells, where it represses the action of a two-repeat MYB gene called *WEREWOLF* (28, 29). In these cases, protein movement involves traversing one or a few cells. If RAD movement is to account for the nonautonomous effects of *RAD*, the effects would either have to occur very early in development (when petals are a few cells wide) or over a longer range than in previously described cases of protein movement.

We thank Minsung Kim, Manuela Costa, and Catherine Baxter for helpful comments on the manuscript and Amelia Green for help with Fig. 3.

1. Stebbins, G. L. (1974) *Flowering Plants: Evolution Above the Species Level* (Harvard Univ. Press, Cambridge, MA).
2. Donoghue, M. J., Ree, R. & Baum, D. A. (1998) *Trends Plant Sci.* **3,** 311–317.
3. Endress, P. (1999) *Int. J. Plant Sci.* **160,** S3–S23.
4. Coen, E. S. (1996) *EMBO J.* **15,** 6777–6788.
5. Luo, D., Carpenter, R., Vincent, C., Copsey, L. & Coen, E. (1996) *Nature* **383,** 794–799.
6. Almeida, J., Rocheta, M. & Galego, L. (1997) *Development (Cambridge, U.K.)* **124,** 1387–1392.
7. Luo, D., Carpenter, R., Copsey, L., Vincent, C., Clark, J. & Coen, E. (1999) *Cell* **99,** 1–12.
8. Galego, L. & Almeida, J. (2002) *Genes Dev.* **16,** 880–891.
9. Cubas, P., Lauter, N., Doebley, J. & Coen, E. (1999) *Plant J.* **18,** 215–222.
10. Stubbe, H. (1966) *Genetik und Zytologie von Antirrhinum L. sect Antirrhinum* (Fischer, Jena, Germany).
11. Carpenter, R. & Coen, E. (1990) *Genes Dev.* **4,** 1483–1493.
12. Hammer, K., Knüpffer, S. & Knüpffer, H. (1990) *Kulturpflanze* **38,** 91–117.
13. Bradley, D., Carpenter, R., Copsey, L., Vincent, C., Rothstein, S. & Coen, E. (1996) *Nature* **379**, 719–797.
14. Coen, E., Carpenter, R. & Martin, C. (1986) *Cell* **47,** 285–296.
15. Ochman, H., Gerber, A. S. & Hartl, D. L. (1988) *Genetics* **120,** 621–623.
16. Simon, R., Carpenter, R., Doyle, S. & Coen, E. (1994) *Cell* **78,** 99–107.
17. Coen, E., Romero, J. M., Doyle, S., Elliott, R., Murphy, G. & Carpenter, R. (1990) *Cell* **63,** 1311–1322.
18. Baur, E. (1924) *Bibl. Genet.* **4,** 1–170.
19. Doyle, S. (1996) Master's thesis (Univ. of East Anglia, Norwich, U.K.).
20. Sommer, H., Hehl, R., Krebbers, E., Piotrowiak, R., Lönnig. W.-E. & Saedler, H. (1988) in *Plant Transposable Elements*, ed. Nelson, O. (Plenum, New York), pp. 227–235.
21. Luo, D., Coen, E., Doyle, S. & Carpenter, R. (1991) *Plant J.* **1,** 59–69.
22. Stracke, R., Werber, M. & Weisshaar, B. (2001) *Curr. Opin. Plant Biol.* **4,** 447–456.
23. Vincent, C. A. & Coen, E. S. (2004) *Can. J. Bot.* **82,** 681–690.
24. Carpenter, R., Copsey, L., Vincent, C., Doyle, S., Magrath, R. & Coen, E. (1995) *Plant Cell* **7,** 2001–2011.
25. Clark, J. I. & Coen, E. S. (2001) *Plant J.* **30,** 639–648.
26. Rose, A., Meier, I. & Wienand, U. (1999) *Plant J.* **20,** 641–652.
27. Nakajima, K., Giovanni, S., Nawy, T. & Benfey, P. N. (2001) *Nature* **413,** 307–311.
28. Wada, T., Kurata, T., Tominaga, R., Koshino-Kimura, Y., Tachibana, T., Goto, K., Marks, M. D., Shimura, Y. & Okada, K. (2002) *Development (Cambridge, U.K.)* **129,** 5409–5419.
29. Lee, M. M. & Schiefelbein, J. (2002) *Plant Cell* **14,** 611–618.